

## Tuning piezoproperties of BiFeO<sub>3</sub> ceramic by cobalt and titanium dual doping

Tuluk, Anton; Joshi, Siddharth; Mahon, Tadhg; Van Der Zwaag, Sybrand

**DOI**

[10.1063/5.0091768](https://doi.org/10.1063/5.0091768)

**Publication date**

2022

**Document Version**

Final published version

**Published in**

Journal of Applied Physics

**Citation (APA)**

Tuluk, A., Joshi, S., Mahon, T., & Van Der Zwaag, S. (2022). Tuning piezoproperties of BiFeO<sub>3</sub> ceramic by cobalt and titanium dual doping. *Journal of Applied Physics*, 131(21), Article 214104. <https://doi.org/10.1063/5.0091768>

**Important note**

To cite this publication, please use the final published version (if applicable).  
Please check the document version above.

**Copyright**

Other than for strictly personal use, it is not permitted to download, forward or distribute the text or part of it, without the consent of the author(s) and/or copyright holder(s), unless the work is under an open content license such as Creative Commons.

**Takedown policy**

Please contact us and provide details if you believe this document breaches copyrights.  
We will remove access to the work immediately and investigate your claim.

***Green Open Access added to TU Delft Institutional Repository***

***'You share, we take care!' - Taverne project***

***<https://www.openaccess.nl/en/you-share-we-take-care>***

Otherwise as indicated in the copyright section: the publisher is the copyright holder of this work and the author uses the Dutch legislation to make this work public.

# Tuning piezoproperties of BiFeO<sub>3</sub> ceramic by cobalt and titanium dual doping

Cite as: J. Appl. Phys. **131**, 214104 (2022); <https://doi.org/10.1063/5.0091768>

Submitted: 17 March 2022 • Accepted: 16 May 2022 • Published Online: 06 June 2022

 Anton Tuluk,  Siddharth Joshi,  Tadhg Mahon, et al.



View Online



Export Citation



CrossMark

## ARTICLES YOU MAY BE INTERESTED IN

[Electric-induced devil's staircase in perovskite antiferroelectric](#)

Journal of Applied Physics **131**, 214105 (2022); <https://doi.org/10.1063/5.0094919>

[Intersubband transitions in nonpolar and semipolar III-nitrides: Materials, devices, and applications](#)

Journal of Applied Physics **131**, 210901 (2022); <https://doi.org/10.1063/5.0088021>

[Investigation of the structural, dielectric, and optical properties of MoSe<sub>2</sub> nanosheets](#)

Journal of Applied Physics **131**, 213101 (2022); <https://doi.org/10.1063/5.0088016>

Journal of Applied Physics **Special Topics** Open for Submissions

[Learn More](#)

# Tuning piezoproperties of BiFeO<sub>3</sub> ceramic by cobalt and titanium dual doping

Cite as: J. Appl. Phys. **131**, 214104 (2022); doi: [10.1063/5.0091768](https://doi.org/10.1063/5.0091768)

Submitted: 17 March 2022 · Accepted: 16 May 2022 ·

Published Online: 6 June 2022



Anton Tuluk,<sup>a)</sup> Siddharth Joshi, Tadhg Mahon, and Sybrand van der Zwaag

## AFFILIATIONS

Novel Aerospace Materials (NovAM), Faculty of Aerospace Engineering, Kluyverweg 1, Delft University of Technology, Delft, the Netherlands

<sup>a)</sup>Author to whom correspondence should be addressed: [A.Tuluk-1@tudelft.nl](mailto:A.Tuluk-1@tudelft.nl)

## ABSTRACT

Bismuth ferrite is a potentially interesting lead-free piezoelectric material for use in high-temperature applications due to its high Curie temperature. However, the high coercive field and high leakage currents of pure BiFeO<sub>3</sub> (BFO) prevent reaching its theoretical performance level. The classic approach to tailoring piezoceramic properties to their desired use conditions is the use of doping. In this work, we produce bulk BFO piezoceramic by the conventional sintering method with single element doping with cobalt (0.125–3 at. %) or titanium (1–5 at. %) and dual doping (Co and Ti added simultaneously). Cobalt doping reduces the required field for poling and also increases the leakage currents. Titanium doping reduces the leakage currents but destroys the piezoelectric properties as the coercive field strength cannot be reached. However, when both elements are used simultaneously at their appropriate levels (0.25 at. % each), a piezoelectric ceramic material is obtained, requiring a low field for full poling (9 kV/mm) and showing excellent room temperature performance such as a  $d_{33} = 40$  pC/N, a dielectric constant in the region of 100 and dielectric losses less than 1%.

© 2022 Author(s). All article content, except where otherwise noted, is licensed under a Creative Commons Attribution (CC BY) license (<http://creativecommons.org/licenses/by/4.0/>). <https://doi.org/10.1063/5.0091768>

## I. INTRODUCTION

For a long time, piezoelectric sensors have been regarded as the most efficient devices for measuring pressure, acceleration, and stress at room temperature. For example, piezoelectric ceramic sensors offer significant advantages over other non-destructive testing methods, such as low cost, ease of operation, and the ability to conduct *in-operando* measurements,<sup>1</sup> but this advantage disappears when the sensor is exposed to high temperatures. The widespread use of piezoelectric ceramics in various applications has become possible due to property tuning via the use of donor or acceptor dopants.<sup>2</sup> Currently, most piezoelectric sensors are based on a modified PZT with the chemical formula:  $\text{PbZr}_x\text{Ti}_{1-x}\text{O}_3$ , which is one of the most widely studied systems from a fundamental and functional point of view but is also a system with no high-temperature application potential. PZT is a perovskite ferroelectric with a cubic symmetry above its Curie temperature and with tetragonal, monoclinic, or rhombohedral distortion in the polar state at lower temperatures, depending on its composition.<sup>3</sup> The ferroelectric or piezoelectric characteristics of the PZT can be tuned toward “hard” or “soft” characteristics by proper doping. The terms “soft”

and “hard” PZT ceramics refer to the minimal field required to achieve a permanently poled state, which in itself depends on the mobility of dipoles or domains, as well as the behavior of polarization and depolarization. “Soft” PZTs are obtained by doping with donor ions such as  $\text{La}^{+3}$  and  $\text{W}^{+6}$  (for site A) and  $\text{Nb}^{+5}$ ,  $\text{Sb}^{+5}$  (for site B), which leads to the creation of vacancies at site A in the lattice.<sup>4</sup> The characteristic features of attractive poling elements are those leading to a relatively high mobility of the domain walls and, as a consequence, a “soft” ferroelectric behavior (easily polarizable). The advantages of “soft” PZT materials are, thus, their large piezoelectric charge constant, moderate dielectric constant, and high coupling factors, which makes them interesting for actuators, sensors such as conventional vibration sensors, ultrasonic transmitters, and receivers for flow or level measurements, electroacoustic applications such as sound transducers and microphones.<sup>5</sup> “Hard” PZT is doped with acceptor ions such as  $\text{K}^{+1}$ ,  $\text{Na}^{+1}$  (for site A) and  $\text{Fe}^{+3}$ ,  $\text{Al}^{+3}$ ,  $\text{Mn}^{+3}$  (for site B), creating oxygen vacancies in the lattice.<sup>6</sup> Such PZT materials can be subjected to high electrical and mechanical stresses, without a change in performance, hence showing good stability. This makes “hard” PZT materials suitable

for high power and high-frequency applications. Other advantages of “hard” PZT ceramics are a moderate dielectric constant value, large piezoelectric coupling factors, and low dielectric losses, which facilitate their further use in the resonant mode only with low internal heating of the component. “Hard” PZT-based piezoelectric elements are used in ultrasonic cleaning, ultrasonic processors, biomedical fields, transducers, hydroacoustic technologies, etc. The large difference in physical properties between “soft” and “hard” groups is mainly due to the contribution of the motion of the domain wall<sup>2,7</sup> and not so much to a change in the crystal lattice values. However, the mechanisms of hardening and softening are not fully understood.

Irrespective of the doping element used to tune the properties of PZT-based piezoelectric sensors, their maximal operating temperatures are around 260 °C or lower due to the intrinsic PZT transformation temperature and the modest effect of doping at that temperature range.<sup>8</sup> Therefore, considerable efforts are now aimed at developing new (i.e., non-PZT based) materials that can satisfy the growing demand for piezoelectric elements with an operating temperature in the range of 350–600 °C. One such material is BiFeO<sub>3</sub> (BFO), with an exceptionally high Curie temperature,  $T_C$ , of 825 °C<sup>9</sup> and the added benefit of having a lead-free composition. This high  $T_C$  makes BFO an ideal candidate for use as a high-temperature lead-free piezoceramic.<sup>1</sup> Unfortunately, research on the bulk ceramics of BFO has not been very successful and did not demonstrate a high piezoelectric coefficient. This was largely due to the problems of electrical leakage and phase purity, which created difficulties in realizing the potential of bulk bismuth ferrite.

As with PZT, one of the ways to solve these problems is to tune the properties of bismuth ferrite by doping. Macroscopic hardening of the ferroelectric behavior of BFO doped up to 3 at. % by Co was recently shown by Makarovic *et al.*<sup>10</sup> In this work, it was shown that the assumptions about p-type conductivity are correct and the main reason for hardening is an increase in the concentration of Co<sub>Fe</sub>-V<sub>O</sub> pinning centers. This mechanism has clear parallels with those in acceptor doped (“hard”) PZT. Continuing the analogy with PZT, it can be assumed that doping with donors such as Ti<sup>4+</sup> should lead to the softening of BFO piezoelectric ceramics due to a decrease in the concentration of pinning centers. No increases in piezoelectric properties and softening were shown for Ti-doped BFO, but only a decrease in  $\tan \delta$  with an increase in the amount of Ti substitution, and this is explained by the assumption that Fe<sup>2+</sup> ions (the predominant cause of high  $\tan \delta$  in BFO) were not formed due to Ti doping.<sup>11,12</sup>

To study the mechanisms of hardening and softening of BFO ceramic, two types of dopants, cobalt and titanium, were chosen. Cobalt concentrations of 0.125, 0.25, and 0.5 at. % were chosen since the concentration of cobalt close to 0.2 at. % leads to an improvement in the ferroelectric and insulating properties of ceramics.<sup>10,13,14</sup> Higher dopant concentrations up to 3 at. % Co have also been tested to ensure that there is an upward trend in conductivity. During the study, it was noticed that doping with cobalt reduces the required poling field to obtain piezoelectric properties in BFO.

To investigate the effect of donor doping on the piezoelectric properties of BFOs, titanium concentrations from 1 to 5 at. % were chosen. When studying the insulating properties of BFO doped with titanium, at higher titanium concentrations, the leakage currents are steadily increasing.<sup>11,15</sup>

Also, the effect of dual doping of cobalt and titanium is investigated and the concentration of doping, in this case, was selected based on the best results of previous experiments. The study has shown that dual doping, with the right concentration selection, allows us to combine the positive effects of separate dopants.

## II. EXPERIMENTAL

BiFeO<sub>3</sub> samples were prepared by a conventional solid-state reaction using analytical grade commercially supplied raw materials: Bi<sub>2</sub>O<sub>3</sub> (99.99% purity), Fe<sub>2</sub>O<sub>3</sub> (99.95% purity), TiO<sub>2</sub> (99.99% purity), and Co<sub>2</sub>O<sub>3</sub> (99.9% purity). All powders were weighed and grounded separately before mixing. Cobalt doping levels were varied between 0.125 and 3 at. %. Titanium doping levels were varied between 1 and 5 at. %. Based on the results of Co- and Ti-doped systems, dual doping levels were chosen as 0.25–0.25, 0.5–0.5, and 0.25–1 at. % Co–Ti. The grinding and mixing processes were performed in isopropanol using yttria-stabilized ZrO<sub>2</sub> balls. The particle size distribution composition of the milled powder is in the range of 0.5–1  $\mu$ m, according to the scanning electron microscope (SEM) images. The powders were dried and calcined at 775 °C for 1 h and at a heating rate of 600 °C/h. Then, the calcined powders were reground, granulated by mixing with 2 wt. % QPAC 40 binder, and uniaxial pressed into disks (13 mm in diameter and 1 mm in thickness) under 200–250 MPa. The pellets were sintered at 800–850 °C for 1 h, depending on their composition. Sintering temperatures were optimized to achieve the best density for a fixed sintering time of 1 h.

Scanning electron microscope (SEM) images of the fracture surfaces were taken using a Jeol JSM-7500F field emission scanning electron microscope. Prior to the SEM measurements, a thin (15 nm) layer of gold was deposited on the sample. Grain size measurement was based on SEM images and the manual evaluation of, typically, 25 grains. To determine the phase purity of various BiFeO<sub>3</sub> systems, x-ray diffraction studies with Cu K $\alpha$  radiation at room temperature were done using a Rigaku Miniflex 600 diffractometer. Given the absence of open porosity, the density was determined by Archimedes’ method in an aqueous medium.

Polarization–electric field hysteresis loops were measured at room temperature by a Radiant precision ferroelectric analyzer at 5 Hz and up to 110 kV/cm (4–5 kV depends on the sample thickness and dielectric strength of samples). For this, gold electrodes were deposited on the ceramics by the magnetron sputtering method. The samples were poled under a DC electric field of 60–110 kV/cm for 20 min in silicone oil at room temperature (due to the risk of electrical breakdown at higher temperatures). The electrical properties of piezoceramics were measured at room temperature using an Agilent 4263B LCR meter at 1 kHz and 1 V, while the piezoelectric properties were measured using a PM300 Berlincourt-type piezometer from Piezotest with a static force of 10 N and a dynamic force of 0.25 N peak-to-peak with a sinusoidal excitation at 110 Hz.

## III. RESULT AND DISCUSSION

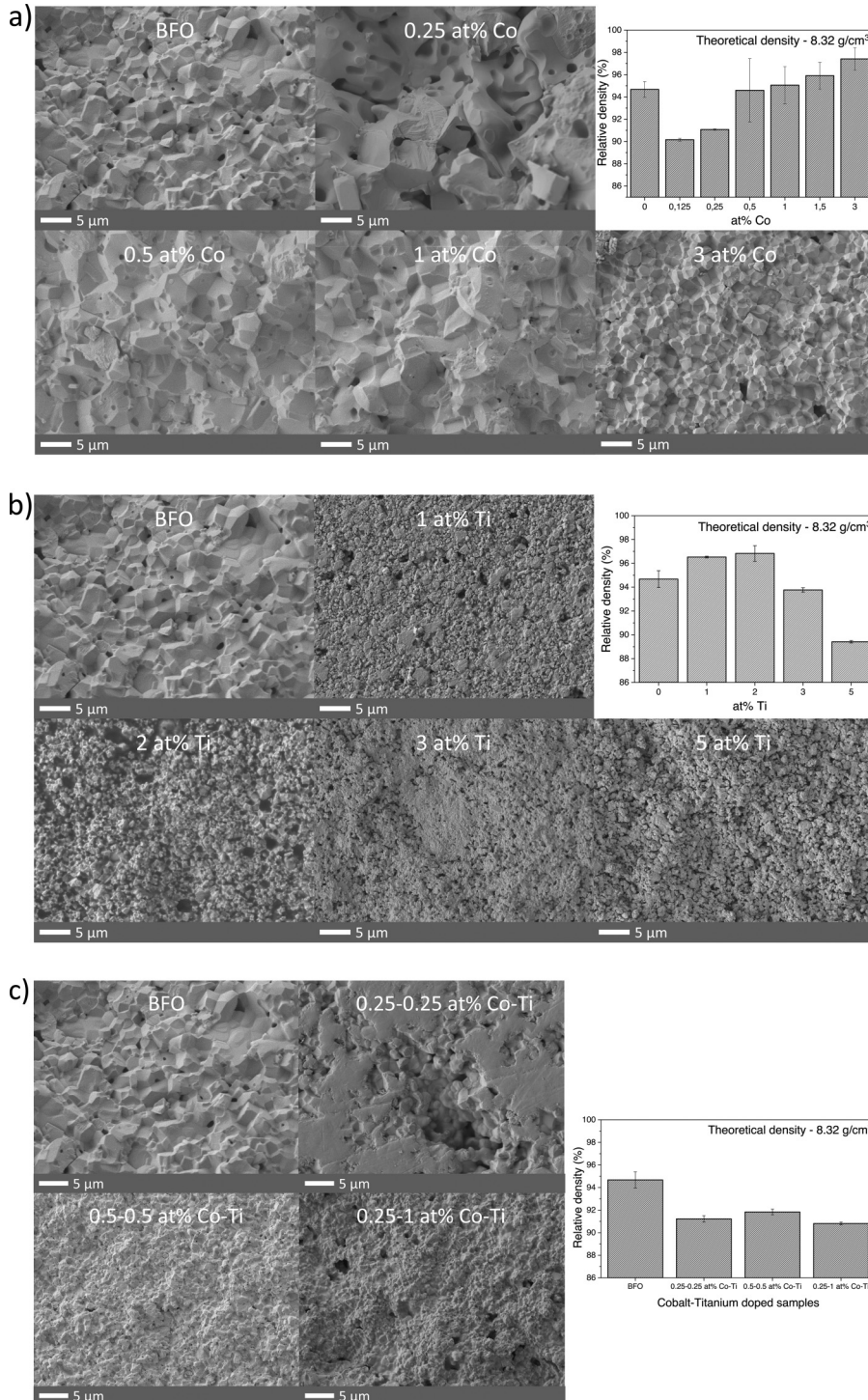
### A. Microstructure

Figure 1 shows SEM images of BFO ceramics, pure and doped with cobalt, titanium, or both, with relative densities reported as well. Macropores are absent in all obtained ceramics. As can be



seen from Fig. 1(a), low concentrations of cobalt (up to 1 at. %) negatively affect the density of ceramics and increase the average grain size. At higher concentrations, the density of the ceramic increases with respect to the undoped BFO.

In contrast, low concentrations of titanium reduce the grain size, while high concentrations of Ti negatively affect the density of the ceramic [Fig. 1(b)]. This effect might be associated with an increase in the concentration of oxygen vacancies, which is



**FIG. 1.** SEM images of fracture surface and relative density in comparison to pure BFO ceramic of representative (a) Co-doped, (b) Ti-doped, and (c) dual-doped BFO samples.

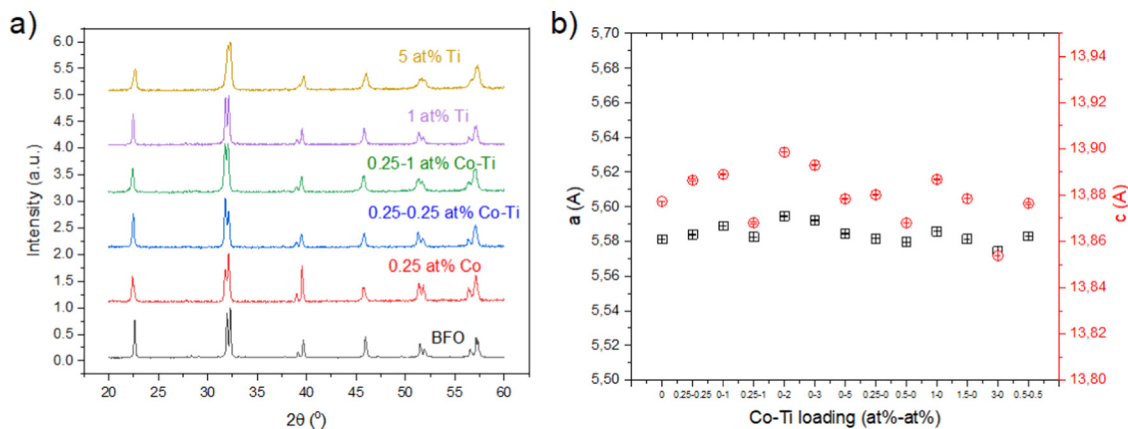


**FIG. 2.** (a) X-ray diffraction pattern of sintered  $\text{BiFeO}_3$  ceramic with different dopants and concentrations and (b) unit cell parameters of their  $R3c$  structure in hexagonal representation obtained by Rietveld refinement.

reported to favorably affect the sintering and growth of ceramic grains.<sup>16</sup>

Figure 1(c) shows the microstructure in dual-doped samples. The effect of titanium on the microstructure of the samples dominates over the effect of cobalt since the grain size decreases in the same way as in the case of doping with titanium only.

## B. Crystal structure

Figure 2(a) shows selected x-ray diffraction patterns of  $\text{BiFeO}_3$  ceramic powder doped by Co, Ti, or both. All materials crystallize in the form of a rhombohedral perovskite structure with space group  $R3c$ . According to the result of Rietveld's refinement (Fig. 1S in the [supplementary material](#)), all systems are practically free of secondary phases. The concentration of the secondary phases of undoped BFO is below 2 wt.% and even lower for the doped systems. The addition of these dopants does not affect the crystal structure, which is reflected in the absence of obvious changes in lattice parameters shown in Fig. 2(b). The differences in peak intensity between the various samples can be attributed to texturing and the differences in grain size for differently doped samples.

## C. Ferroelectric

As shown in many other works on bismuth ferrite,<sup>10,13,17</sup> undoped bismuth ferrite has a high coercive field and demonstrates a pinched ferroelectric loop. In our case, as shown in Fig. 3, the ferroelectric loop is clamped and only opens when a high field of 120 kV/cm in combination with a high temperature is reached. This may be due to an increase in the mobility of defects at elevated temperatures. A pinched hysteresis loop is often observed when the state of a ferroelectric domain wall is characterized by random internal electric fields. In our case, this may be due to the high oxygen vacancy content which forms defective dipoles.

Ferroelectric hysteresis loops for pure and cobalt-doped ceramics are shown in Fig. 4(a). All loops, except for pure BFO, have a pinched shape characteristic of BFO ceramics.<sup>13,14</sup> The

addition of cobalt in our case does not lead to the hardening of BFO, as happens in the case of PZT, but rather leads to the opposite effect.

Figure 4(b) shows that the leakage currents increase with an increase in the cobalt concentration, which can also be associated with an increase in the concentration of oxygen vacancies. Several published experimental and theoretical studies demonstrate that unmodified BFO-based ceramics exhibit p-type ( $\text{Fe}^{4+}$ ) conductivity when sintered in the air.<sup>13,18–21</sup> According to a recent defect chemical model,<sup>22</sup> an increase in electrical conductivity in the range of 0.125–3 at.% Co [see Fig. 4(b)] can be explained by an increase in the concentration of electron holes ( $\text{Fe}^{4+}$ ). Samples with a doping concentration of 1.5 and 3 at.% Co show electrical breakdown at fields above 10 kV/cm. The results show that Co acts as an acceptor

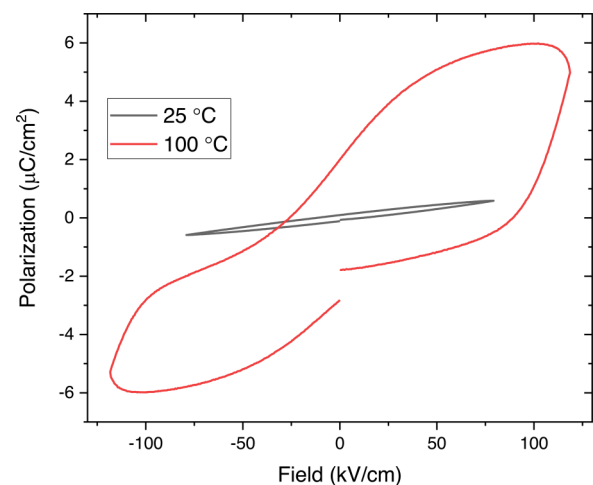


**FIG. 3.** Ferroelectric hysteresis loops of pure BFO ceramic samples at two temperatures.

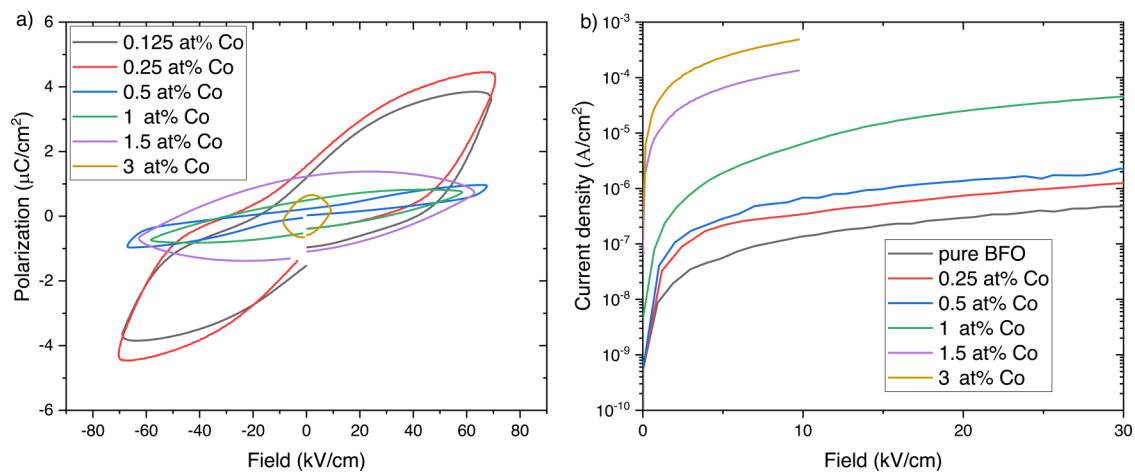
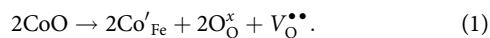


FIG. 4. (a) Ferroelectric hysteresis loops and (b) leakage current density of Co-doped BFO ceramic samples.

dopant according to the defect response in Eq. (1), where the  $\text{Co}^{2+}$  acceptor replacing the  $\text{Fe}^{3+}$  position in BFO is supposed to compensate for the charge with oxygen vacancies ( $V_{\text{O}}^{\bullet\bullet}$ ),



Considering that the concentration of  $V_{\text{O}}^{\bullet\bullet}$  is closely related to the valence state of Fe, an increase in the concentration of  $V_{\text{O}}^{\bullet\bullet}$  due to doping with Co will increase the p-type conductivity.

Leakage currents and ferroelectric loops of titanium-doped samples are shown in Fig. 5. For all concentrations, the loops do not open, not even for the highest field values of 150–160 kV/cm. If we consider the softening and hardening mechanisms inherent in PZT, we would expect to see the opposite result when doping with a donor such as titanium. But as we can see, all ferroelectric

and piezoelectric properties disappear. Leakage currents for the Ti-doped samples decrease until reaching a minimum at 2 at. % Ti concentration and then increase back with a subsequent increase in Ti concentration (until 5 at. %) but still lower than the undoped samples. This may be the result of a significant reduction in oxygen vacancies and the prevention of  $\text{Fe}^{4+}$  formation. Consequently, the dominant charge compensation mechanism in  $\text{Ti}^{4+}$  doped BFO is the filling of oxygen vacancies,<sup>12</sup> although the creation of some  $\text{Fe}^{2+}$  ions or  $\text{Fe}^{3+}$  vacancies cannot be ruled out. Oxygen and iron ions are usually immobile at room temperature. Ionic conduction supported by the field can be due to the transfer of electrons between neighboring  $\text{Fe}^{2+}$  and  $\text{Fe}^{3+}$  ions in a strong field so that the  $\text{Fe}^{2+}$  ions actually jump forward against the applied field.

The above results may be further evidence that oxygen vacancies are the main cause of high leakage current in undoped BFO,

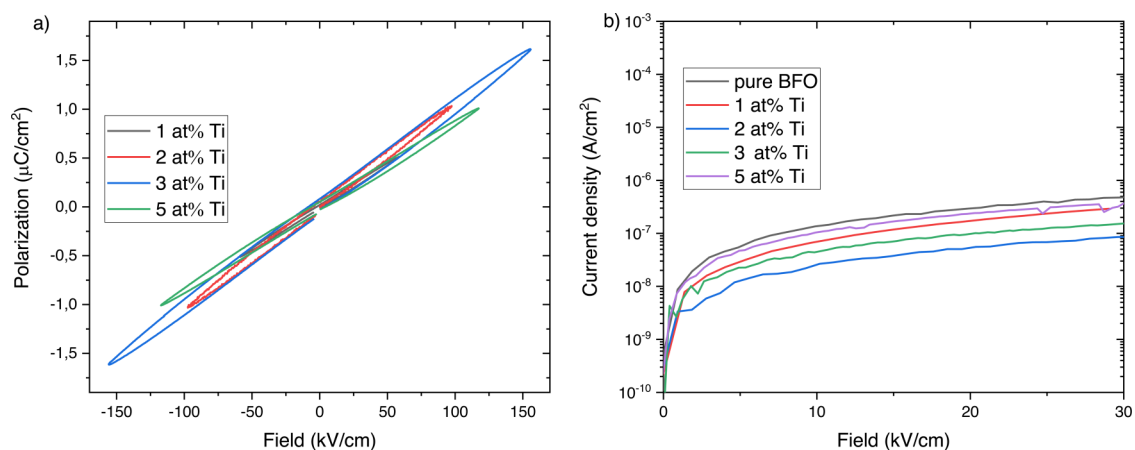


FIG. 5. (a) Ferroelectric hysteresis loops and (b) leakage current density of Ti-doped BFO ceramic samples.



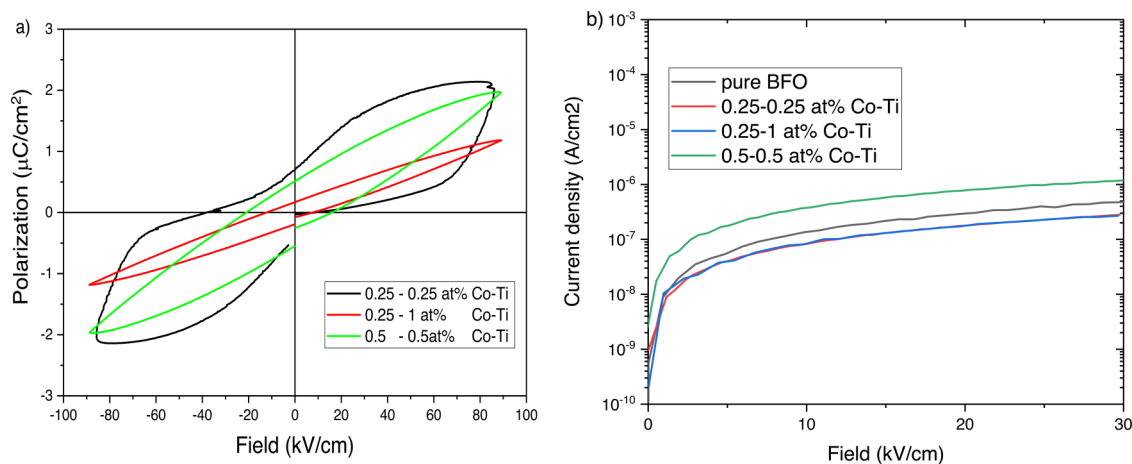


FIG. 6. (a) Ferroelectric hysteresis loops and (b) leakage current density of Co-Ti dual-doped BFO ceramic samples.

and doping with higher valence ions reduces DC conductivity. However, this result can also be associated with a change in the microstructure since the grain size decreases with titanium doping, which can also lead to a decrease in conductivity.

Ferroelectric loops and leakage currents of samples doped with cobalt and titanium are shown in Fig. 6. At low concentrations of titanium and cobalt, it is possible to combine the positive aspects of both dopants: a decrease in the coercive field, due to cobalt, and a decrease in leakage current, due to titanium. With an increase in the titanium concentration, the leakage currents decrease even more but this also leads to a strong increase in the coercive field. For a sample with 0.5–0.5 at. % Co-Ti, it can be seen that the effect of cobalt to increase conductivity dominates over the effect of adding titanium.

#### D. Piezoelectric

Table I shows the piezoelectric and electrical properties of undoped and doped BFO samples. All samples were polarized at the maximum field ( $E_p$ ) at which no electrical breakdown occurs yet. As always, the piezoelectric properties of materials are dependent on their insulating properties, which limit the maximum poling field that can be applied.

Thus, the low piezoelectric properties of undoped BFO can be explained by the high coercive field and the inability to reach it due to high leakage currents. Increasing the temperature during poling greatly increases the risk of electrical breakdown and cannot be used due to the damage to the samples. As we can see, with an increase in the concentration of cobalt, due to an increase in leakage current, the dielectric strength of the material also decreases, which leads to a decrease in the maximum field  $E_p$  that can be applied. However, at low concentrations of cobalt, this did not interfere with successful polarization of the ceramics and led to a piezoelectric coefficient of 43 pC/N being achieved for samples with 0.25 at. % Co.

On the other hand, doping with titanium at low concentrations increases the dielectric strength of the samples in comparison with that of undoped BFO. But even with polarization at 130 kV/cm, piezoelectric properties were not obtained. With a subsequent increase in the concentration of titanium, the dielectric strength still decreases but at higher concentrations compared to cobalt.

The results obtained are inconsistent with the typical behavior of piezoelectric ceramics upon doping with donors and acceptors and demonstrate opposite results, such as softening upon doping with a donor and hardening upon doping with an acceptor. In this regard, the results with samples doped with cobalt are of particular interest since, despite the fact that leakage currents inevitably increase, the piezoelectric properties increase significantly. However, with a further increase in the concentration of cobalt, the

TABLE I. Summary of piezoelectric and electrical properties at room temperature.

Composition	$E_p$ (kV/cm)	$d_{33}$ (pC/N)	$\epsilon_r$ (–)	$\tan \delta$ (–)
BFO	100	9	80	0.005
BFO 0.125 at. % Co	60	40	70	0.008
BFO 0.25 at. % Co	60	43	80	0.017
BFO 0.5 at. % Co	60	36	80	0.033
BFO 1.0 at. % Co	30	...	80	0.166
BFO 1.5 at. % Co	10	...	100	0.458
BFO 3.0 at. % Co	10	...	130	0.939
BFO 1 at. % Ti	130	1	100	0.006
BFO 2 at. % Ti	110	1	110	0.006
BFO 3 at. % Ti	60	...	110	0.007
BFO 5 at. % Ti	60	...	115	0.007
BFO 0.25–0.25 at. % Co-Ti	90	40	95	0.009
BFO 0.25–1 at. % Co-Ti	90	2	100	0.014
BFO 0.5–0.5 at. % Co-Ti	90	5	100	0.018

piezoelectric constant again decreases to zero, because we cannot impose a polarization field higher than the coercive field. An increase in piezoelectric properties by doping BFO with Co can be described as a softening of piezoelectric ceramics and a decrease in the coercive field, which some authors associate with an increase in the mobility of domain walls with an increase in their conductivity,<sup>23</sup> whereas Ti doping, which reduces all types of conductivity and the grain size of the ceramics, leads to a result where the coercive field increases even more, which completely destroys the effective piezoelectric properties.

Dual doping with cobalt and titanium, while maintaining the effect of reducing the required field to obtain piezoelectric properties, also reduces the dielectric loss of the resulting ceramic. The proposed explanation is that cobalt presumably binds oxygen vacancies near the domain walls, increasing their conductivity, and hence, mobility, whereas titanium evenly distributed throughout the sample reduces the overall conductivity of the BFO. By optimizing the concentration of both dopants, we managed to achieve a piezoelectric constant of 40 pC/N with dielectric losses below 1%.

These results show that the correct manipulation of defects in the BFO ceramics allows the tuning of piezoelectric and electrical properties, which in the future may allow the use of these ceramics at elevated temperature conditions, given its high Curie temperature—in case the high electrical conductivity at high temperatures can be mitigated.

#### IV. CONCLUSION

In this work, we studied the effect of doping BFO with cobalt and titanium on the electrical conductivity and piezoelectric properties. We found that doping with cobalt leads to a decrease in the coercive field of the piezoelectric ceramic and an increase in electrical conductivity. This effect is presumably associated with an increase in the concentration of oxygen vacancies due to the acceptor nature of doping. The decrease in the coercive field of piezoceramics makes it possible to achieve the maximum possible piezoelectric constant in the region of 43 pC/N with a relatively small polarizing field in the region of 60 kV/cm.

Doping with titanium leads to a decrease in conductivity, which can be explained by a decrease in the concentration of oxygen vacancies. Also, doping with titanium significantly reduces the piezoelectric properties of BFO.

Dual doping with cobalt and titanium combines the positive effects of both dopants, such as a decrease in the coercive field for polarization, and an increase in the insulating properties of the material. When both elements are used simultaneously at their appropriate levels (0.25 at. % each), a piezoelectric ceramic material is obtained that requires a low field for full poling (90 kV/cm) and shows excellent room temperature performance such as a  $d_{33} = 40$  pC/N, a dielectric constant in the region of 100 and dielectric losses less than 1%.

#### SUPPLEMENTARY MATERIAL

Rietveld's refinement results and the grain size of pure and doped BFO samples can be found in the [supplementary material](#).

#### AUTHOR DECLARATIONS

##### Conflict of Interest

The authors have no conflicts to disclose.

#### DATA AVAILABILITY

The data that support the findings of this study are available from the corresponding author upon reasonable request.

#### REFERENCES

- <sup>1</sup>T. Stevenson, D. G. Martin, P. I. Cowin, A. Blumfield, A. J. Bell, T. P. Comyn, and P. M. Weaver, *J. Mater. Sci. Mater. Electron.* **26**, 9256–9267 (2015).
- <sup>2</sup>S. Takahashi, *Ferroelectrics* **41**, 143–156 (1982).
- <sup>3</sup>A. S. Bhalla, R. Guo, and R. Roy, *Mater. Res. Innovat.* **4**, 3–26 (2000).
- <sup>4</sup>V. D. Kugel and L. E. Cross, *J. Appl. Phys.* **84**, 2815–2830 (1998).
- <sup>5</sup>N. Horchidan, C. E. Ciomaga, R. C. Frunza, C. Capiani, C. Galassi, and L. Mitoseriu, *Ceram. Int.* **42**, 9125–9132 (2016).
- <sup>6</sup>M. I. Morozov and D. Damjanovic, *J. Appl. Phys.* **107**, 034106 (2010).
- <sup>7</sup>E. M. Bourim, H. Tanaka, M. Gabbay, G. Fantozzi, and B. L. Cheng, *J. Appl. Phys.* **91**, 6662 (2002).
- <sup>8</sup>M. J. Schulz, M. J. Sundaresan, J. McMichael, D. Clayton, R. Sadler, and B. Nagel, *J. Intell. Mater. Syst. Struct.* **14**, 693–705 (2003).
- <sup>9</sup>R. Palai, R. S. Katiyar, H. Schmid, P. Tissot, S. J. Clark, J. Robertson, S. A. T. Redfern, G. Catalan, and J. F. Scott, *Phys. Rev. B* **77**, 1 (2008).
- <sup>10</sup>M. Makarovic, N. Kanas, A. Zorko, K. Ziberna, H. Ursic, D. R. Smabraton, S. M. Selbach, and T. Rojac, *J. Eur. Ceram. Soc.* **40**, 5483–5493 (2020).
- <sup>11</sup>G. D. Hu, S. H. Fan, C. H. Yang, and W. B. Wu, *Appl. Phys. Lett.* **92**, 90 (2008).
- <sup>12</sup>X. Qi, J. Dho, R. Tomov, M. G. Blamire, and J. L. MacManus-Driscoll, *Appl. Phys. Lett.* **86**, 1 (2005).
- <sup>13</sup>T. Rojac, A. Bencan, B. Malic, G. Tutuncu, J. L. Jones, J. E. Daniels, and D. Damjanovic, *J. Am. Ceram. Soc.* **97**, 1993–2011 (2014).
- <sup>14</sup>J. Walker, H. Ursic, A. Bencan, B. Malic, H. Simons, I. Reaney, G. Viola, V. Nagarajan, and T. Rojac, *J. Mater. Chem. C* **4**, 7859–7868 (2016).
- <sup>15</sup>S. J. Kim, S. H. Han, H. G. Kim, A. Y. Kim, J. S. Kim, and C. Il Cheon, *J. Korean Phys. Soc.* **56**, 439–442 (2010).
- <sup>16</sup>R. D. Levi and Y. Tsur, *Adv. Mater.* **17**, 1606–1608 (2005).
- <sup>17</sup>T. Rojac, M. Kosec, B. Budic, N. Setter, and D. Damjanovic, *J. Appl. Phys.* **108**, 074107 (2010).
- <sup>18</sup>E. Markiewicz, B. Hilczer, M. Błaszzyk, A. Pietraszko, and E. Talik, *J. Electroceram.* **27**, 154–161 (2011).
- <sup>19</sup>D. Maurya, H. Thota, K. S. Nalwa, and A. Garg, *J. Alloys Compd.* **477**, 780–784 (2009).
- <sup>20</sup>M. I. Morozov, M.-A. Einarsrud, and T. Grande, *J. Appl. Phys.* **115**, 044104 (2014).
- <sup>21</sup>T. Rojac, A. Bencan, G. Drazic, N. Sakamoto, H. Ursic, B. Jancar, G. Tavcar, M. Makarovic, J. Walker, B. Malic, and D. Damjanovic, *Nat. Mater.* **16**, 322–327 (2017).
- <sup>22</sup>E. T. Wefring, M.-A. Einarsrud, and T. Grande, *Phys. Chem. Chem. Phys.* **17**, 9420–9428 (2015).
- <sup>23</sup>M. Makarovic, M. Ç. Bayir, H. Ursic, A. Bradesko, and T. Rojac, *J. Appl. Phys.* **128**, 064104 (2020).